As an illustration, in Table 1 the values of the peak factor for BPSK are presented, while in Table 2 the values of the peak factor for QPSK are shown.

BER penalty: In the process of reducing the PF, the amplitude of $s^{(m)}(t)$ for some m has been reduced. As a consequence the BER of $x_1(t)$ will increase. This is in fact the price paid for the reduction of the PF. In Fig. 1*a* curves of BER for BPSK against SNR are shown: the broken line shows the BER for $x(t)$, while the solid line shows the BER for $x_1(t)$. The SNR penalty at $BER = 10^{-4}$ is ~1, 2 and 2.5dB for N = 4, 8 and 12, respectively.

Conclusion: A method for MCM with low peak factor is presented for which the net bit rate remains the same as for standard MCM. However the BER is slightly higher than that in standard MCM. This BER degradation may be effectively improved by using FEC.

The proposed method is very simple for on-line implementation: it is required only to measure the maximal value of the modulated signal for each symbol, and then to attenuate or amplify the signal accordingly.

The off-line calculation of the value of the PF is very time consuming for large N.

© IEE 1996

11 June 1996

Electronics Letters Online No: 19961258

D. Wulich (*Communications Laboratory, Department of Electrical and Computer Engineering, Ben-Gurion University of the Negev, Beer-Sheva 84105, Israel*)

References

1 JONES, A.E., WILKINSON, T.A., and BARTON, S.K.: 'Block coding scheme for reduction of peak to mean envelope power ratio of multicarrier transmission schemes', *Electron. Lett.*, 1994, **30**, pp. 2098–2099

2 WULICH, D.: 'Reduction of peak to mean ratio of multicarrier modulation by cyclic coding', *Electron. Lett.*, 1996, **32**, pp. 432–433

3 SHEPHERD, S.J., VAN EEVELT, P.W.J., WYATT-MILLINGTON, C.W., and BARTON, S.K.: 'Simple coding scheme to reduce peak factor in QPSK multicarrier modulation', *Electron. Lett.*, 1995, **31**, pp. 1131–1132

4 BOYD, S.: 'Multitone signals with low crest factor', *IEEE Trans.*, 1986, **CAS-33**, pp. 1018–1022

5 VAN EETVELT, P.W.J., SHEPHERD, S.J., and BARTON, S.K.: 'The distribution of peak-factor in QPSK multi-carrier modulation', *Wirel. Pers. Commun.*, 1995, **2**, pp. 87–96

6 WULICH, D.: 'Some properties of peak to average power ratio of BPSK modulated multicarrier signal', submitted to *IEEE Trans. Commun.*

Practical consideration for bandpass sampling

Ronggang Qi, F.P. Coakley and B.G. Evans

Indexing terms: Digital communication systems, Sampling theory

The uniform bandpass sampling theorem has been modified to cope with sampling frequency instability and carrier frequency variations. Minimum sampling rates for given sampling and carrier frequency variations are derived. A robust bandpass sampling method is proposed which requires the sampling frequency to be such that the carrier frequency is on the 1/4 or –1/4 sampling frequency grid.

Introduction: The sampling of bandpass signals is often encountered in digital communication systems. To sample a bandpass signal it is usually down-converted to a frequency band near zero frequency with an analogue mixer (or pair of mixers for quadrature sampling), then sampled at a low Nyquist rate. Alternatively, it can be sampled directly at sampling frequencies lower than the Nyquist rate according to the first-order bandpass sampling theory [1, 2]. For a single-side-band (SSB) signal centred at the carrier frequency f_c with one-sided bandwidth B, the required theoretical minimum sampling rate is [3, 4]

$$f_s^{(min)} = (2f_c + B)/I \qquad (1)$$

where $I = \lfloor f_c/B + 0.5 \rfloor$ ($\lfloor\cdot\rfloor$ denotes the floor function). The minimum sampling rates are graphically shown by the upper edge of the dark shaded area in Fig. 1, in which the sampling and the carrier frequencies are normalised by B, and $1/2 \le \sigma \le 1/2$. It has been shown that sampling at frequencies higher than the theoretical minimum does not necessarily guarantee aliasing-free sampling, unless the following condition is met [5, 6]:

$$(2f_c + B)/n \le f_s \le (2f_c - B)/(n-1) \qquad (2)$$

where n, $1 \le n \le I$, is referred to as the wedge order. The $n = 1$ case is obviously the Nyquist sampling rate, while $n = I$ corresponds to the minimum sampling rate. Eqn. 2 defines I wedge-shaped non-contiguous operating regions of aliasing-free sampling. In between, there are I–1 disallowed regions shown as lightly shaded areas in Fig. 1.

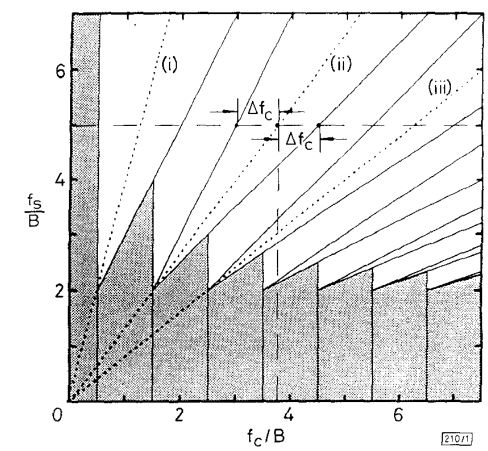

Fig. 1 *Minimum and acceptable sampling frequencies*

$f_c/B = I + \sigma$
(i) $n = 1$
(ii) $n = 2$
(iii) $n = 3$

Direct bandpass sampling takes advantage of eliminating the use of analogue mixer(s), hence is free of the DC offset effect introduced by analogue mixer(s) and, for quadrature bandpass sampling, free of mismatch of gain and phase between I and Q channels due to non-ideal mixers and A/D converters. It tends however to be sensitive to variations in both the carrier and the sampling frequencies.

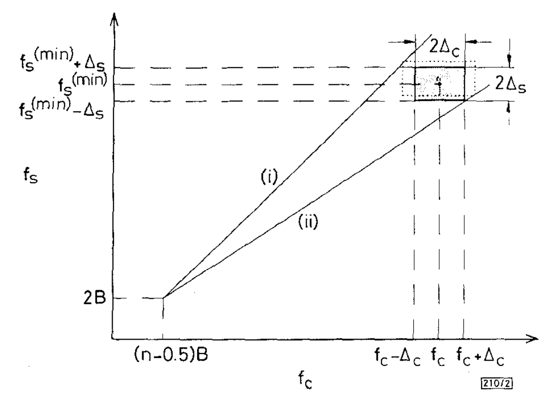

Fig. 2 *Operation region in nth wedge*

(i) $f_s = (2f_c - B)/(n - 1)$
(ii) $f_s = (2f_c + B)/n$

Practical consideration of minimum sampling rates: The minimum sampling rate of eqn. 1 does not take into account the instability of the sampling and carrier frequencies, which would pull the operating point away from the allowed region, causing aliasing. To modify eqn. 1, consider the nth wedge of the allowed region in Fig. 1. The wedge is confined by two intersecting lines, $f_s = (2f_c - B)/(n-1)$ and $f_s = (2f_c + B)/n$, where $f_c \geq (n - 0.5)B$. Instead of requiring a single operating point (f_c, f_s) being within the wedge, a neighbouring area (shown as the shaded rectangle in Fig. 2 and defined by Δ_c and Δ_s which are, respectively, the deviations of f_c and f_s due to their uncertainties) should be within the wedge for aliasing-free sampling. The minimum sampling frequency in the wedge $f_s^{(min)}(n)$ can be determined by letting the lower right corner of the rectangle on the lower edge and the upper left corner below the upper edge of the wedge as shown in Fig. 2, i.e.

$$f_s^{(min)}(n) - \Delta_s \leq [2(f_c + \Delta_c) + B]/n \qquad (3)$$

$$f_s^{(min)}(n) + \Delta_s \leq [2(f_c - \Delta_c) - B]/(n-1) \qquad (4)$$

In practice, Δ_s is usually given in terms of the relative precision (stability) of f_s: $\Delta_s = p_s f_s$, (e.g. $p_s = 10^{-3}$ for a moderate RC oscillator and $p_s = 10^{-5}$ for a crystal). From eqns. 3 and 4, for given f_c, Δ_c, and p_s, to minimise $f_s^{(min)}(n)$, the largest n must be used. Hence

$$f_s^{(min)} = f_s^{(min)}(I') = \frac{2(f_c + \Delta_c) + B}{I'(1 - p_s)} \qquad (5)$$

where

$$I' = \left\lfloor \frac{(1 + p_s)(2(f_c + \Delta_c) + B)}{4(f_c p_s + \Delta_c) + 2B} \right\rfloor \qquad (6)$$

Clearly, the theoretical minimum sampling rate of eqn. 1 is a special case of eqns. 5 and 6 with $p_s = \Delta_c = 0$.

Maximum tolerance to carrier frequency variations: In radar, sonar, and mobile satellite communication systems the received bandpass signals are subjected to the Doppler effects causing offsets in the carrier frequencies. Other than requiring the minimum sampling rate for given sampling frequency stability and carrier frequency variation, for these applications, we can slightly relax the sampling frequency while maximising the tolerance to the carrier frequency variation, as long as a minimum guard band is satisfied. In so doing, we fix the height of the rectangle in Fig. 2 and let its width be variable, and then move it along the vertical line 'f_c = the carrier frequency' until it is equally divided by the line and is tangential to the wedge (the dotted rectangle shown in Fig. 2). Thus in this case, eqn. 3 still holds whereas eqn. 4 takes the equal sign.

The sampling frequency and the guard band can be therefore determined by

$$f_s = \frac{4f_c}{2n - 1 - p_s} \qquad (7)$$

$$\Delta_c = \frac{2(1 - (2n-1)p_s)f_c - (2n - 1 - p_s)B}{2(2n - 1 - p_s)} \qquad (8)$$

Since $2n-1 > p_s$, from eqn. 7, the carrier and the sampling frequency are approximately related by

$$f_c \simeq \begin{cases} (J + 1/4)f_s & J = (n-1)/2 \quad \text{for } n \text{ odd} \\ (J - 1/4)f_s & J = n/2 \quad \text{for } n \text{ even} \end{cases} \qquad (9)$$

eqn. 9 defines a set of lines intersecting at the origin (dotted lines in Fig. 1). Besides the main advantage of being tolerant to carrier frequency uncertainty, the $^1/4f_s$ (or $-^1/4f_s$) stacking of carrier can also reduce computations in digital (Hilbert) processing [2] and lead to a multiplierless frequency shifter for spectral manipulations.

Example: Consider a real SSB bandpass signal centred at f_c = 140MHz with B = 12.5MHz, which requires a theoretical minimum sampling frequency of 25.455MHz (eqn. 1). Assuming $p_s = 10^{-4}$ and Δ_c = 900kHz, the practical minimum sampling frequency can be determined as $f_s^{(min)}$ = 29.433MHz using eqns. 5 and 6. If high tolerance to carrier variation is desired, then f_s = 29.474MHz according to eqn. 9, which gives Δ_c = 1.104MHz.

Conclusions: The theoretical minimum sampling rate for bandpass signals needs to be modified when sampling frequency instability and carrier frequency uncertainty are taken into account. The modified uniform bandpass sampling theorem is more practical for engineering use. Tolerance to sampling frequency variation and carrier uncertainty is maximised if the operating region in the nth wedge is tangential to the wedge edges and the operating point is at the centre of the region, which leads to $^1/4f_s$ (for n odd, or $-^1/4f_s$ for n even) stacking of carrier. In addition, it also has the advantage of simplifying digital processing and allowing a simple quadrature sampler structure to be used.

© IEE 1996
29 April 1996
Electronics Letters Online No: 19961244

Ronggang Qi, F.P. Coakley and B.G. Evans (*Centre for Satellite Engineering Research, University of Surrey, Guildford, Surrey GU2 5XH, United Kingdom*)

References

1 WATERS, W.M., and JERRETT, B.R.: 'Bandpass signal sampling and coherent detection', *IEEE Trans.*, 1982, **AES-18**, (4), pp. 731–736
2 RICE, D.W., and WU, K.H.: 'Quadrature sampling with high dynamic range', *IEEE Trans.*, 1982, **AES-18**, (6), pp. 736–739
3 FELDMAN, C.B., and BENNETT, W.R.: 'Bandwidth and transmission performance', *Bell Syst. Tech. J.*, 1949, **28**, pp. 490–595
4 GREGG, W.D.: 'Analog and digital communication' (John Wiley & Sons, New York, 1977)
5 VAUGHAN, R.G.: 'The theory of bandpass sampling', *IEEE Trans.*, 1991, **SP-39**, (9), pp. 1973–1984
6 GASKELL, J.D.: 'Linear systems, Fourier transforms, and optics' (Wiley, New York, 1978)

Rapid DTMF signal classification via parallel cascade identification

M.J. Korenberg and P.W. Doherty

Indexing terms: Keyboards, Pattern classification, Signal processing, Telephone equipment

The parallel cascade identification of nonlinear systems is used for the rapid recognition of dual tone multi-frequency (DTMF) signals, i.e. the 'dual tones' used to encode the digits on a telephone keypad. The authors demonstrate that parallel cascades can correctly identify DTMF signals with half or less than half of the input data required by current methods.

Introduction: The parallel cascade identification [1] of nonlinear systems has already been successfully used to identify and classify a variety of signals. In this Letter, we focus on the rapid recognition of standard telephony DTMF signals. Since DTMF was first introduced in the 1960s as a replacement for dial pulse signalling, its use has expanded to include such applications as remote data entry, voice mail, and automated attendant positions. The primary benefit of DTMF over dial pulse is increased efficiency, as a result of reduced holding times for signal detection and recognition hardware. Rapid identification of DTMF signals will reduce holding times further, greatly increasing the service capacity of DTMF receivers.

DTMF signals are characterised by the superposition of two sinusoidal tones; these signals consist of one tone each from the high (1209, 1336, 1477, and 1633Hz) and low (697, 770, 852, and 941Hz) groups of frequencies. Accurate identification of the 16 possible digits thus requires distinguishing between frequencies separated by as little as 127Hz in the high band, and 73Hz in the low band.

Current DTMF detection and classification methodology, while for the most part proprietary, relies primarily on one or more of the following techniques: narrowband digital filtering [2], spectral analysis via discrete Fourier transform [3], and counting zero/extrema crossings [4]. Each of the above methodologies has an inherent latency required to determine the correct received signal (i.e. recognise the DTMF digit). This latency ranges from a low of 40–50 samples for digital filters (following lowpass filtering of the input signal), to 150–200 samples for zero/extrema crossings. A standard sampling frequency of 8kHz is assumed for all methodologies.